An Open Loop Space Vector PWM Control for CSI-fed Field-Oriented Induction Motor Drive with Improved Performances and Reduced Pulsating Torque

LEILA. MOUSSAOUI [1], **Prof. AMMAR. MOUSSI** [2]
Department of Electrotechnique, Faculty of Engineering,
[1] University of Setif (19000), ALGERIA, [2] University of Biskra (07000), ALGERIA.
[1] Email: leila_moussaoui@hotmail.com, [2] Email: moussi_am@hotmail.com

Abstract: - An induction machine, fed by an auto-sequentially current source inverter (CSI) with semiconductors having turn-off capability was investigated. An indirect field oriented control (IFOC) is proposed for controlling the drive speed. However the speed performance control can be deteriorate by the severe pulsating nature of induction motor torque at very low speed. In order to achieve precise torque control with reduced pulsating torque and minimized speed vibration, space current vector modulation (SVPWM or SVM) has been proposed.

The SVM is a performant open loop current vector modulation strategy. Compared with the sinusoidal PWM (SPWM), this provides large inverter capacity and better harmonic characteristics. Simulation results with the two PWM strategies's are given and discussed. It is concluded the proposed control based on SVM schemes produced better performances in both high and low speed with preserve of the good dynamic performance of FOC. It also allows reducing the switching losses while achieving low levels of torque ripple that are comparable with the torque ripple produced by the SPWM at a higher switching number.

Key-Words: - induction motor, space vector modulation, current source inverter, torque ripple, vector control.

1 Introduction

To deal with the advances of the power electronics and microprocessors, the induction motor used in variable speed drive and position servo control have become more and more attractive because of their simplicity, rugged structure, low maintainability, and economy etc. In Addition, induction motor can be controlled like DC motor using space vector field-oriented control approach [1], [2].

Usually, induction motors are fed by voltage source inverters (VSI), mainly because VSI have faster current response and can be applied easily to a PWM system in the high-frequency region due to its low impedance. The CSI, however, still has better features, such as capability of four-quadrant operation without any extra power circuit for regeneration, ruggedness and reliability. With CSI, high precision current control is possible. Thus, CSI seem to be more appropriate for large capacity drive systems such as steel mills, elevator motors, and so on [1, 5-9]. However, at low speeds of operation, the conventional current source inverter produces undesired torque pulsations, due the presence of harmonics in the rectangular current waveform. This time variant harmonic torques and the associated rotor speed oscillations inherent in a rectifier-inverter induction motor drive system are objectionable in applications such as machine tool and antenna positioning, where uniform speed is mandatory [1, 2, 6, 7, 10-12].

Presently used techniques, aimed at reducing the pulsation torque in a current source inverter fed motor drive, are based on reduction of the harmonics present in the motor current. Common examples of such methods are: 1) the improvement of current wave shape by current superposing method using multiple current source inverters, 2) the current instantaneous value control method and 3) the current-pulse width modulation (PWM) method [3, 6, 13].

PWM approach is one of the best techniques used in power inverters to obtain controllable ac output. Among of PWM methods, the sine-triangle or sinusoidal PWM strategy (SPWM) which was particularly suitable for early analogue pulse-width modulators [3, 14-16].The Space Vector PWM or space vector modulation (SVPWM or SVM) is another popular and widely used PWM strategy and is more preferable scheme for instantaneous current control since it gives a large linear control range, less harmonics distortion and fast transient response. It has also higher DC bus utilisation and reduced switching losses as compared to the sine-triangle intersection technique. Besides, it is well suited to

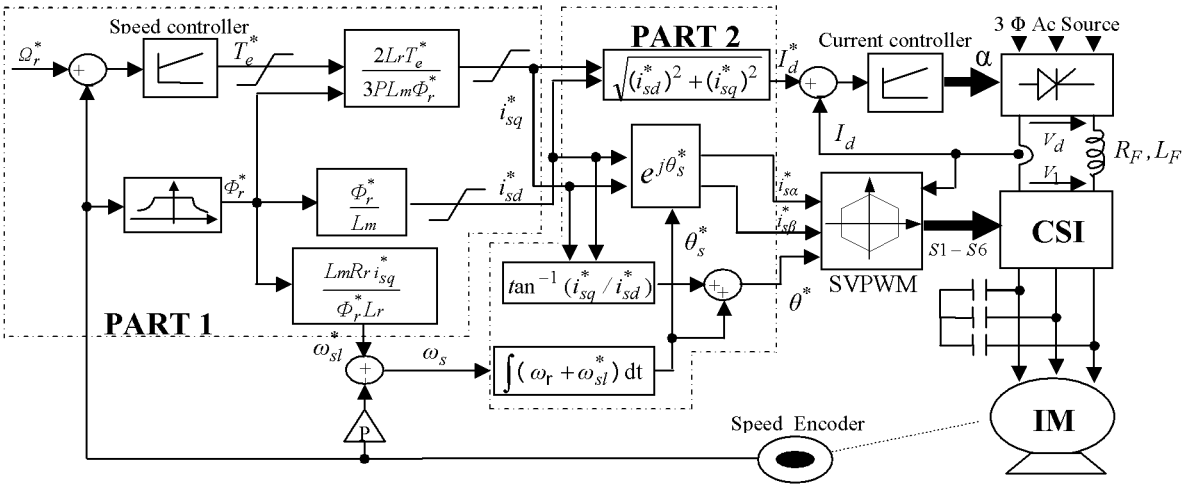

Fig. 1. The proposed control scheme's bloc diagram.

digital implementation. SVM also aligns better with field oriented control technique, where improved dynamic response is achieved [4, 9, 14, 17, 24, 25].

This paper brings out the principles involved in the generation of PWM waveforms based on the Space Vector approach. Different SVM schemes used for an open loop control of indirect field-oriented-IM fed by current source inverter, have been compared to each other and to the SPWM by means of computer simulation, based then on different merit factors; such as the total harmonic distortion in the output current waveform, switching losses, RMS current ripple, or torque ripple.

2 System Structure

The drive system complete block diagram which includes a speed controller employing field oriented control is shown in Fig.1.

2.1 Machine Model

The electrical dynamics of an induction motor in the synchronously rotating reference frame can be expressed, [3, 18], as

$$\begin{bmatrix} R_s+L_\sigma p & \omega_s L_\sigma & \frac{L_m}{L_r}p & \omega_s\frac{L_m}{L_r} \\ -\omega_s L_\sigma & R_s+L_\sigma p & -\omega_s\frac{L_m}{L_r} & \frac{L_m}{L_r}p \\ -R_r\frac{L_m}{L_r} & 0 & \frac{R_r}{L_r}+p & (\omega_s-\omega_r) \\ 0 & -R_r\frac{L_m}{L_r} & -(\omega_s-\omega_r) & \frac{R_r}{L_r}+p \end{bmatrix} \begin{bmatrix} i_{sq} \\ i_{sd} \\ \Phi_{rq} \\ \Phi_{rd} \end{bmatrix} = \begin{bmatrix} V_{sq} \\ V_{sd} \\ 0 \\ 0 \end{bmatrix} \quad (1)$$

where :

V_{sd} , V_{sq}	d and q axis stator voltages,
$i_{sd}, i_{sq}, i_{rd}, i_{rq}$	d and q axis stator and rotor currents,
R_s , R_r	stator and rotor resistances,
L_s , L_r	stator and rotor inductances,
$L_m, L_\sigma = \frac{L_s L_r - L_m^2}{Lr}$	mutual and leakage inductances,
P	number of poles pairs,
ω_s, ω_r	electrical and rotor angular velocity,
ω_{sl}	slip angular frequency,

The developed electromagnetic torque is given by

$$Te = \frac{3}{2}\frac{P}{2}\frac{L_m}{L_r}\cdot\left(\Phi_{rd}\cdot i_{sq} - \Phi_{rq}\cdot i_{sd}\right) \quad (2)$$

with

$$\begin{aligned} \Phi_{rd} &= L_r.i_{rd} + L_m.i_{sd} \\ \Phi_{rq} &= L_r.i_{rq} + L_m.i_{sq} \end{aligned} \quad (3)$$

The two rotor equations corresponding to the third and fourth row of equation (1) can be rewritten as

$$-R_r\frac{L_m}{L_r}i_{sq} + (\frac{R_r}{L_r}+p)\Phi_{rq} + \omega_{sl}\Phi_{rd} = 0 \quad (4)$$

$$-R_r\frac{L_m}{L_r}i_{sd} - \omega_{sl}\Phi_{rq} + (\frac{R_r}{L_r}+p)\Phi_{rd} = 0 \quad (5)$$

2.2 Indirect Field-Oriented Control

For field-oriented control, the instantaneous speed of rotor flux vector is selected to revolve at the synchronous speed, and the d axis is aligned. Then, the q axis component of the rotor flux vanishes and the rotor flux Φ_r is entirely in the d axis, i.e.,

$$\Phi_{rq} = p\Phi_{rq} = 0 \quad (6)$$

and

$$\Phi_{rd} = \Phi_r = constant \quad (7)$$

Substituting equations (6) and (7) into equations (4), (5) and (2) yields

$$\omega_{sl}^* = \frac{R_r L_m}{\Phi_r^* L_r} i_{sq}^* \quad (8)$$

$$i_{sd}^* = \frac{\Phi_r^*}{L_m} \quad (9)$$

$$i_{sq}^{*} = \frac{2L_r}{3PL_m \Phi_r^{*}} T_e^{*} \qquad (10)$$

From equation (10), if rotor flux Φ_r^{*} is kept constant for the constant torque operation, the electromagnetic torque T_e^{*} can be linearly varied by adjusting i_{sq}^{*}. Therefore, the induction machine is controlled like a separately excited dc machine using field-oriented control method.

2.3 Current Source Inverter

The CSI is supplied by a phase-controlled rectifier at the front end and the dc voltage of the rectifier is adjusted by a closed-loop current control. Fig.1 shows that a proportional-integral (PI) controller is used in the current-feedback control loop. At the rectifier level, an inverse-cosine firing-angle control scheme is used.

The PWM-CSI allows simultaneous conduction on the same phase legs, while only one of three devices on the same side is conducted. At the output of the inverter, a three-phase ac capacitor is needed, acting as a filter together with the inductor. The dc inductor also serves as an energy storage element, so that a boosted voltage can be achieved at the output [23].

Fig. 2 left reveals the diagram of the CSI. Where the semiconductors are considered as ideal switches and the switching rules are as follow:

- Due to the dc-link inductance L_F, the dc-current I_d must never be interrupted.
- The distribution of the dc-current I_d into the three phases a, b and c must not depend on the load.

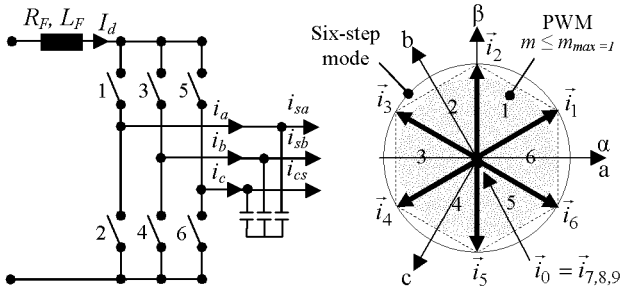

Fig. 2. Left: model of the inverter
Right: switching states of the inverter currents

According to these rules, exact one of the upper and one of the lower switches must be closed all the time. This results in nine allowed switching states (table 1). Three of them (7, 8, 9) are zero states. Since their effects are equal, they are designated homogeneously as state 0. These seven different vectors of the inverter currents $\vec{i}$ are shown in Fig. 2 right and they are defined as:

$$\vec{i}_k = \frac{2}{\sqrt{3}} I_d \exp \mathrm{j}\left(\frac{k\pi}{3} - \frac{\pi}{6}\right)$$
$$\vec{i}_{k+1} = \frac{2}{\sqrt{3}} I_d \exp \mathrm{j}\left(\frac{k\pi}{3} + \frac{\pi}{6}\right) \qquad k = 1, 2, \ldots\ldots 6 \qquad (11a)$$

$$\vec{i}_0 = \vec{i}_{7,8,9} \qquad (11b)$$

Switch N° 1 2	3 4	5 6	Phase currents i_a	i_b	i_c	Current Vector $\vec{i}_k$	Name
1 0	0 0	0 1	I_d	0	$-I_d$	$(2I_d e^{(j\pi/6)})/3^{1/2}$	$\vec{i}_1$
0 0	1 0	0 1	0	I_d	$-I_d$	$(2I_d e^{(j\pi/2)})/3^{1/2}$	$\vec{i}_2$
0 1	1 0	0 0	$-I_d$	I_d	0	$(2I_d e^{(j5\pi/6)})/3^{1/2}$	$\vec{i}_3$
0 1	0 0	1 0	$-I_d$	0	I_d	$(2I_d e^{(j7\pi/6)})/3^{1/2}$	$\vec{i}_4$
0 0	0 1	1 0	0	$-I_d$	I_d	$(2I_d e^{(j3\pi/2)})/3^{1/2}$	$\vec{i}_5$
1 0	0 1	0 0	I_d	$-I_d$	0	$(2I_d e^{(j11\pi/6)})/3^{1/2}$	$\vec{i}_6$
1 1	0 0	0 0	0	0	0	0	$\vec{i}_7$
0 0	1 1	0 0	0	0	0	0	$\vec{i}_8$
0 0	0 0	1 1	0	0	0	0	$\vec{i}_9$

Table 1: states of the inverter

2.4 Space Vector Modulation Strategy

It is well known that SVM is produced by the regular-sampling of a circular locus of a reference current in the two-axis reference frame. These current samples are then represented by two actives vectors, chosen from $\vec{i}_1 \rightarrow \vec{i}_6$, adjacent to the reference current sample together with either all the null vectors; $\vec{i}_7, \vec{i}_8,$ and $\vec{i}_9$, or only one null vectors; $\vec{i}_7$ or $\vec{i}_8$ or $\vec{i}_9$, by adjusting their respective times within a sample period [14, 19-22,24-27].

Fig. 3(a) shows the principle; where the reference vector $\vec{i}_s^{*}$ is sampled at the fixed and equal intervals of time T_s, called 'subcycle'. The sampled value $i_s^{*}(t_s)$ is then used to solve the equations:

$$T_k \vec{i}_k + T_{k+1} \vec{i}_{k+1} = T_s \, i_s^{*}(t_s) \qquad (12a)$$
$$T_0 = T_s - T_k - T_{k+1} = T_{7,8,9} \qquad (12b)$$

where $\vec{i}_k$ and $\vec{i}_{k+1}$ are the two switching state vectors adjacent in space to the reference vector $\vec{i}_s^{*}$, Fig. 3(b).

The solutions of (11) and (12) are the respective on-durations $T_k, T_{k+1},$ and T_0 of the switching state vectors $\vec{i}_k, \vec{i}_{k+1}, \vec{i}_0$:

$$T_k = \left(\cos\left((k-1)\frac{\pi}{3}\right) i_{s\alpha}^{*} + \sin\left((k-1)\frac{\pi}{3}\right) i_{s\beta}^{*}\right) \frac{T_s}{I_d} \qquad (13a)$$

$$T_{k+1} = \left(\cos\left((k+1)\frac{\pi}{3}\right) i_{s\alpha}^{*} + \sin\left((k+1)\frac{\pi}{3}\right) i_{s\beta}^{*}\right) \frac{T_s}{I_d} \qquad (13b)$$

$$T_0 = T_s - T_k - T_{k+1} = T_{7,8,9} \qquad (13c)$$

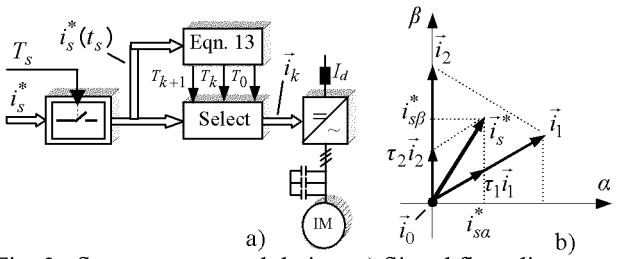

Fig. 3. Space vector modulation; a) Signal flow diagram, b) Switching state vectors of the first 60°-sector

Selecting the appropriate non-zero current vector relies on the phase angle θ^* witch can be divided into six areas in a circle as following:

$$\frac{(k-1)\pi}{3} < \theta_k^* \le \frac{k\pi}{3}, \qquad \text{for k = 1, 2, 3, 4, 5, 6} \quad (14)$$

where θ^* is the phase angle between $\vec{i}_s^*$ and the fixed as-axis expressed as: (included in Part 2 of Fig. 1)

$$\theta^* = \theta_s^* + \tan^{-1}(i_{sq}^* / i_{sd}^*) \quad (15)$$

2.5 Selection of the Switching Sequence

The degrees of freedom we have in the choice of a given modulation algorithm, are:

1) The choice of the zero vector (whether we would like to use $\vec{i}_7$ or $\vec{i}_8$ or $\vec{i}_9$ or all of them).
2) Sequencing of the vectors.
3) Splitting of the duty cycles of the vectors without introducing additional commutations.

The following section will analyse three modulation schemes which can be subdivided in two categories; symmetrical and asymmetrical SVM. Theses schemes are described for the case when the reference vector is in sector 1: all other cases are circularly symmetric.

2.5.1 Symmetrically Generated SVM

This modulation scheme is based on symmetrical sequence within each sampling period. The two following switching mode will satisfy the criteria:

$$- \ \vec{i}_1 \Rightarrow \vec{i}_2 \Rightarrow \vec{i}_9 \Rightarrow \vec{i}_2 \Rightarrow \vec{i}_1 \quad \text{(SVM-1)}$$

$$- \ \vec{i}_1 \Rightarrow \vec{i}_2 \Rightarrow \vec{i}_8 \Rightarrow \vec{i}_2 \Rightarrow \vec{i}_1 \quad \text{(SVM-2)}$$

where only one zero vector is applied in between two active vectors $\vec{i}_k$ and $\vec{i}_{k+1}$ adjacent to the reference current vector $\vec{i}_s^*$ as shown in Fig. 4 for two sampling periods.

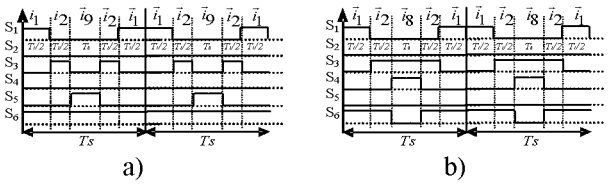

Fig. 4. Timing diagram of : a) SVM-1, b) SVM-2

2.5.2 Asymmetrically Generated SVM

In this technique, the state current vectors are arranged such that the number of switching within one subcycle is minimized. According to this rule, two switching schemes are proposed.

- Scheme 1

In this scheme, both the active current vectors are there in-between two zero current space vectors. Therefore, three possible switching modes can be presented for example in two sectors (1 and 2) as follows:

$$- \ \vec{i}_9 \Rightarrow \vec{i}_1 \Rightarrow \vec{i}_2 \Rightarrow \vec{i}_9 \ \rightarrow \ \vec{i}_8 \Rightarrow \vec{i}_2 \Rightarrow \vec{i}_3 \Rightarrow \vec{i}_8 \quad \text{(SVM-3)}$$

$$- \ \vec{i}_9 \Rightarrow \vec{i}_1 \Rightarrow \vec{i}_2 \Rightarrow \vec{i}_8 \ \rightarrow \ \vec{i}_8 \Rightarrow \vec{i}_2 \Rightarrow \vec{i}_3 \Rightarrow \vec{i}_7 \quad \text{(SVM-4)}$$

$$- \ \vec{i}_7 \Rightarrow \vec{i}_1 \Rightarrow \vec{i}_2 \Rightarrow \vec{i}_7 \ \rightarrow \ \vec{i}_7 \Rightarrow \vec{i}_2 \Rightarrow \vec{i}_3 \Rightarrow \vec{i}_7 \quad \text{(SVM-5)}$$

One disadvantage of the last mode e.g., SVM-5 is that the zero vectors are anuniformly distributed and the timing diagram shown in Fig. 5(c) (for two sampling periods) is not the same for all sectors.

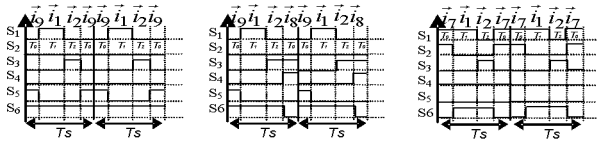

Fig. 5. Timing diagram of : a) SVM-3, b) SVM-4, c) SVM-5

- Scheme 2

A modified version of the symmetrical SVM schemes is used here with usually the same aim of reducing the number of commutations. This can be achieved by the two following sequence over time T_s as illustrated in Fig. 6.

$$- \ \vec{i}_1 \Rightarrow \vec{i}_2 \Rightarrow \vec{i}_8 \quad \text{(SVM-6)}$$

$$- \ \vec{i}_1 \Rightarrow \vec{i}_2 \Rightarrow \vec{i}_9 \quad \text{(SVM-7)}$$

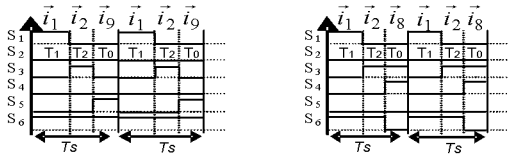

Fig. 6. Timing diagram of : a) SVM-7, b) SVM-6

2.6 Comparison of Switching Sequences

The switching performance of all schemes described in this work are summarised in table 2. According to this table and the previous discussion, SVM-7 renders the minimum number of commutations and states within T_s. So SVM-7 has the lowest switching frequency and hence results in minimum switching losses.

In order to have an objective comparison of the drive unit; all switching schemes have been operating on the drive system and simulation results have show to be favourable for all these schemes with approximately the same ripple levels in current waveforms and the consequent electromagnetic torque.

Switching sequence	N° switching within *Ts*	Dominant harmonics	N° states
SVM-1	8	*Fs=1/Ts*	5
SVM-2	8	*Fs*	5
SVM-3	6	*Fs/2*	4
SVM-4	10	*Fs/2*	4
SVM-5	8	*Fs/2*	4
SVM-6	8	*Fs/2*	3
SVM-7	6	*Fs/2*	3

Table 2

Thus, the SVM-7 seems to be the best switching sequence with minimum loss under open loop space vector PWM control.

3 Simulation results

A computer simulation was performed for the proposed drive system shown in Fig. 1 to evaluate the performance of the proposed SVM schemes using the software package of MATLAB/ SIMULINK. To show the effectiveness of the proposed SVPWM control, the performance is compared with that of the SPWM control studies in the previous work [3].

By considering only the best switching sequence of SVM schemes e.g., SVM-7 with sampling time T_s = 0.001s, system responses of both PWM control are shown in Fig. 7 and Fig. 8 for a speed command of 100 rad/s. With no load, these figures indicate that both PWM methods have no distinct difference between transient and steady-state responses of speed, torque, and stator/dc-link current. However, in the case of SVM schemes, one can see from Fig. 8 that the d-q axis currents are controlled separately or very much decoupled. In contrast, with the SPWM the d-q axis currents are bad decoupled which deteriorate the basic performance of the FOC.

In order to verify the dynamic behaviour of the two methods, a step variation from 0 to 12 Nm has been applied to torque command at 0.5 s. Simulation results included in figures 7 and 8 shows that this causes a small decrease in the speed and good dynamic performances for both PWM methods.

For more utilisation, of SVM schemes, one can see from table 1 that the magnitude of the active vectors is $2/\sqrt{3}\,I_d$. Therefore the dc link current can be kept constant with reduced value evaluated as:

$$I_d^* = \frac{\sqrt{3}}{2}\left|i_s^*\right| \qquad (16)$$

By using the SVM-7 with reduced dc link current in the control of the drive system, simulation results given in Fig. 9 show that, the reduction of dc link current does not deteriorate the good dynamic performance of basic SVM schemes.

For a close inspection of steady state performances, a comparison of steady state behaviours obtained using the two PWM control schemes is shown respectively in Fig. 10-11, Fig. 12-13 and Fig. 14-15 for SPWM, SVM-7, and SVM-7 with reduced dc-link current. Where for all, the machine is running at low speed (10 rad/s) with no load. It is possible to see in figures 10-13, a comparable results in terms of current waveform distortion, torque ripple and speed vibration have been obtained using both PWM strategy's.

From the locus current given in Fig. 13(c), one can see an appreciable reduction in current ripple level

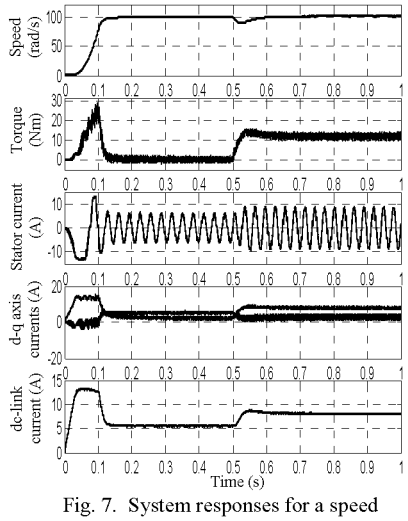

Fig. 7. System responses for a speed command of 100 rad/s with SPWM

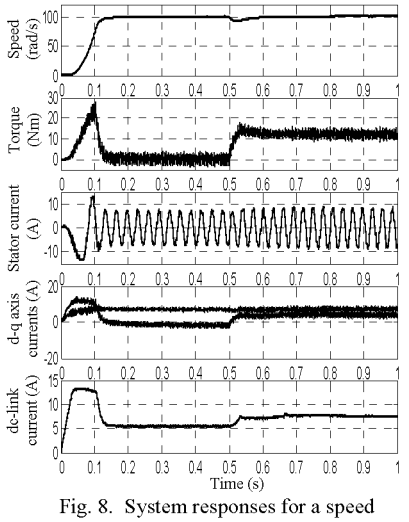

Fig. 8. System responses for a speed command of 100 rad/s with SVM-7

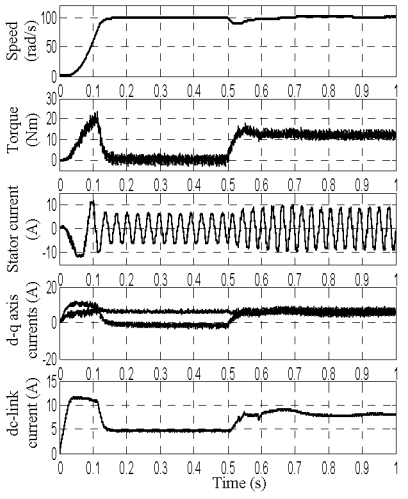

Fig. 9. System responses for a speed command of 100 rad/s with SVM-7 under reduced dc-link

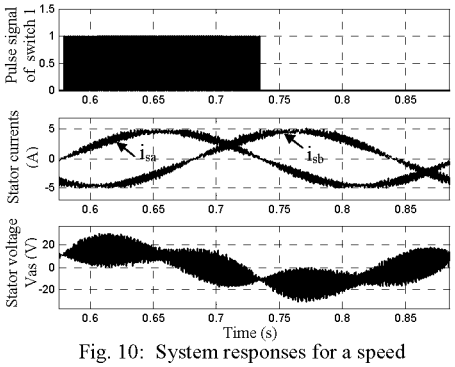

Fig. 10: System responses for a speed command of 10 rad/s and SPWM strategy.

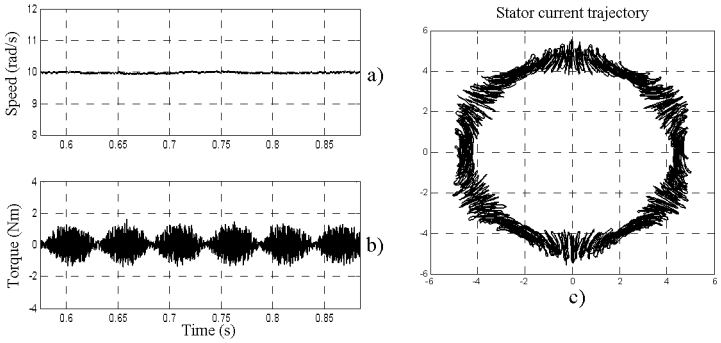

Fig. 11: a) speed response, b) developed torque and c) stator current trajectory for a speed command of 10 rad/s and SPWM strategy.

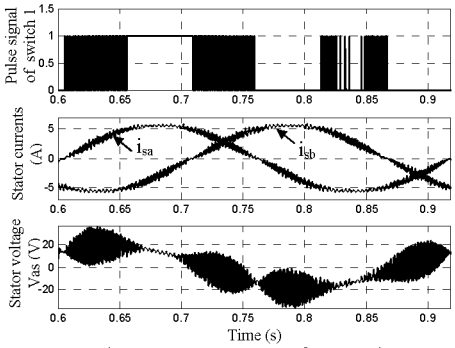

Fig. 12. System responses for a speed Command of 10 rad/s and SVM-7 scheme.

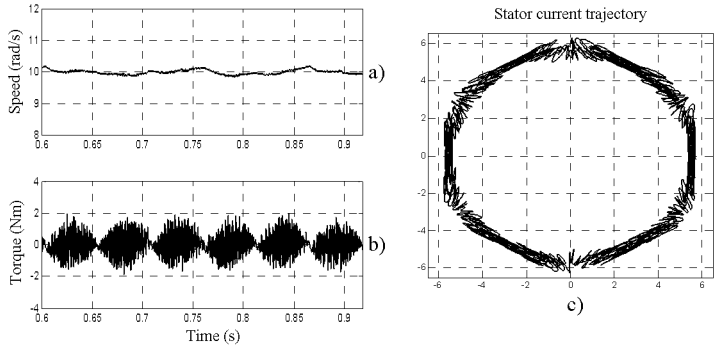

Fig. 13. a) speed response, b) developed torque and c) stator current trajectory for a speed command of 10 rad/s and SVM-7 scheme.

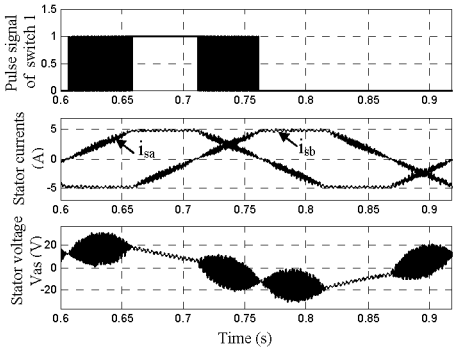

Fig. 14. System responses for a speed command of 10 rad/s and SVM-7 under reduced dc-link current.

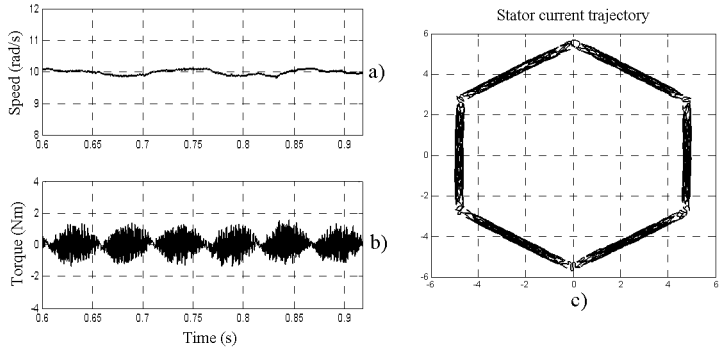

Fig. 15. a) speed response, b) developed torque and c) stator current trajectory for a speed command of 10 rad/s and SVM-7 under reduced dc-link current.

with the need of less switching number which occurs in the case of using SVM-7 as shown in Fig. 12. Where the zero vector is uniformly distributed, with high dc-link utilisation more than the SPWM strategy, (Fig. 10 and Fig. 11(c)).

In addition, The proposed control scheme (SVM-7) with reduced dc-link current, can achieve the switching number with more reduction than SPWM and basic SVM. It has been verified that even in this case the SVM technique allows the torque ripple and speed vibration to be reduced as well as with trapezoidal current waveform as it is clearly observed in Fig. 14 and Fig. 15.

4 Conclusion

The aim of the computer simulations was a search for a drive control system with good performance properties in the case of PWM current source inverter supplying an induction motor under field oriented control. Thus the modelling simulation and analysis of vector controlled induction motor with speed PI controller are describes.

Different space current vector modulation schemes have been proposed and compared to the SPWM strategy. Simulation results have proved the feasibility and the validity of the proposed SVM method and shows that these SVM schemes improves the torque control characteristic in both high and low speed region. It also gives good performance as well as SPWM method in terms of current/torque ripple and speed vibration.

As it is deduced from simulation results; although

torque harmonics are produced by the harmonics currents; there is no stringent relationship between both of them. Lower torque ripple can go along with higher current harmonics, and vice versa. Therefore, for more reduction of torque pulsations a closed loop torque control is required with current vector selection using switching table.

Appendix

Induction motor parameters

Power	4 kw	Stator leakage inductance	0.121 H
Stator voltage	200 v	Rotor leakage inductance	0.121 H
Number of poles	2	Mutual inductance	0.1198 H
Stator resistance	2.4 Ω	Rotor resistance	1.452 Ω
Inertia	0.013 Kg.m^2	friction coefficient	0.002 Nm/rd/s

References

[1] Bose. B.K,*Power Electronics and Ac Drives.* Englewood Cliffs, NJ: Prentice-Hall 1987.

[2] Vladan. P, *Modelling and Minimization Of Torque Ripple In Permanent Magnet Synchronous Motors.* M.S. Thesis, May 28, 1998, Northeastern University.

[3] Moussaoui. L., Moussi. A, Performances Assessment of Field-Oriented Control and Torque Ripple Reduction for CSI-Fed Induction Motor with PWM Strategy's. *3ème Conf sur le GE, EMP, Alger, 15-16 Février 2004.*

[4] Marwali. N.M, Keyhani. A, Tjanaka. W, Implementation of Indirect Vector Control on an Integrated Digital Signal Processor-Based System. *IEEE Trans on EC*, Vol. 14, No. 2, June 1999, pp.139-146.

[5] Chang-Huan. L., Ying-Fang. F, Modelling and Implementation of a Microprocessor–Based CSI-Fed Induction Motor Drive Using Field-Oriented Control. *IEEE Trans. IA*, Vol .25, No.4, July/August. 1989, pp.588-597.

[6] Gopakumar. K., Vithayathil. J, Modified Current Source Inverter fed Induction Motor Drive with Reduced Torque Pulsations. *IEE Proceeding*. Vol. 131, Pt. B. No. 4, July 1984, pp.159-164.

[7] Panda. A.K., Patra. K.C., Duttagupta. P.B, A Comparative Study of Torque Pulsations in Induction Motor with CSI and VSI Drives. *Jour of the Instit of Engineers, India*, No. 78, March 1998, pp.182-188.

[8] Mirafzal. B., Demerdash. N.A.O, A nonlinear controller for current source inverter induction motor drive systems. *IEMDC'03. IEEE International* , Vol. 3, 1-4 june 2003, pp.1491 - 1497

[9] Eichenberger. P., Junger. M, Predictive Vector Control of Stator Voltages for an Induction Machine Drive with Current Source Inverter. *IEEE* 1997, pp.1295-1301.

[10] Grieve. D.W., Mcshane. I.E, Torque Pulsations on Inverter Fed Induction Motors. *4th INCEMD*, No. 310, 1989, pp. 328-333, London.

[11] Leonhard. W, *Control of Electrical Drives.* Braunschweig, May 1996.

[12] Ide. K., Bai. Z.G, vector approximation method with parameter adaptation and torque control of CSI-fed induction motor. *IEEE Trans on IA*, Vol. 31, No. 4, July/August 1995, pp. 830-840.

[13] Chin. T.H., Tomita. H, The principles of Eliminating Pulsating Torque in Current Source Inverter Induction Motor Systems. *IEEE Trans on IA*, Vol. IA-17, No. 2, March/April 1981, pp.160-166.

[14] Narayanan. G., Ranganathan. V.T, Synchronised PWM Strategies Based on Space Vector Approach. Part1: Principles of Waveform Generation. *IEE Proc.-Electr. PA.*, Vol. 146. No. 3, May 1999, pp.267-275.

[15] Nystrom. A., Hylander. J., Thorborg. K, Harmonic Currents and Torque Pulsations with Pulse Width Modulation Method in AC Motor Drives. *3th International Conf on PE and V S drives. London,* UK. No. 291, 1988, pp.378-381.

[16] Zhou. K., Wang. D, Relationship between space-vector modulation and three-phase carrier-based PWM: a comprehensive analysis [three-phase inverters]. *IEEE Trans on IE*, Vol. 49, Feb. 2002, pp.186 – 196.

[17] Bowes. S.R., Grewal. S, Novel Harmonic Elimination PWM Control Strategies for Three-Phase PWM Inverters Using Space Vector Techniques. *IEE Proc.-Electr. PA.*, Vol. 146, No. 5., Sept 1999, pp.495-514.

[18] Huang. C.Y., Chen. T.C, A Microcomputer-Based Induction Motor Drive System Using Current and Torque Control. *IEEE Trans on EC*, Vol. 14, No. 4, December 1999, pp. 874-880.

[19] Lascu. A.M. Trzynadlowski. N, Combining the principles of sliding mode, direct torque control, and space-vector modulation in a high-performance sensorless AC drive. *IEEE Trans on IA*, Vol.40, Jan.-Feb. 2004, pp.170 – 177.

[20] Foussier. P, *Contribution à L'intégration des Systèmes de Commande des Machines Electrique à Courant Alternatif.* Thèse doct., Institut National des Sciences Appliqués de LYON, 1998.

[21] Himamshu. V.P, *Analysis and Comparison of Space Vector Modulation Schemes for Three-Leg and Four-Leg Voltage Source Inverters.* M.S. Thesis, Virginia Polytechnic Institute and State University. May 15, 1997.

[22] Moussaoui. L., Moussi. A, Performances Improvement and Torque Ripple Attenuation in CSI-Fed Field-Oriented Induction Motor Drive Based on Space Cur-rent Vector Modulation. *Premier Congrès Interna-tional sur le Génie Electrique (CIGE'04)*, 10-12 Octobre 2004, pp. 221-225, Sétif, Algérie.

[23] Yin. Y., Wu. A.Y, A Low- Harmonic Electric Drive System Based on Current-Source Inverter. *IEEE TRANS on IA.*, Vol.34, No.1, January/February 1998, pp.227-235.

[24] Dorin O. N, Space Vector Modulation- An Introduction. *IECON'0,* 2001, pp.1583-1592.

[25] Henriksen. S.J., Betz. R.E., Cook. B.J, Digital Hardware Implementation of a Current Controller for IM Variable Speed Drives. *IEEE.* 1998, pp.609-616.

[26] Tripathi. A.M., Khambadkone. S.K.P, Stator Flux Based Space-Vector Modulation and Closed Loop Control of the Stator Flux Vector in Overmodulation Into Six-Step Mod. *IEEE Trans on PE*, Vol.19, May 2004, pp.775 – 782.

[27] Barro. R., Hsu. P, Torque Ripple Compensation of Vector Controlled Induction Machines. *IEEE* 1997, pp.1281-1287.